P102 MOBILE RADAR AND DAMAGE ASSESSMENT OF THE 24 MAY 2011, CANTON LAKE, OKLAHOMA TORNADO

Karen A. Kosiba, Joshua Wurman, Paul Robinson
Center for Severe Weather Research, Boulder, Colorado
Christopher Schwarz
University of Oklahoma, Norman, Oklahoma
Donald Burgess
Cooperate Institute for Mesoscale Meteorological Studies, Norman, Oklahoma
Ted Mansell
National Severe Storms Laboratory
Daniel Dawson
National Severe Storms Laboratory,
University of Oklahoma,
Cooperate Institute for Mesoscale Meteorological Studies Norman, Oklahoma

1. INTRODUCTION

The DOW7 (Wurman et al. 1997; Wurman 2001) and NOXP (Palmer et al. 2009) mobile radars collected data on an EF3 tornado that occurred near Canton Lake, OK on 24 May 2011. Peak winds measured by DOW7 were ~80 m s^{-1} at a height of 45 m above ground level and ~85 m s^{-1} by NOXP. An extensive ground-based damage survey was conducted immediately following the event, which resulted in the EF3 rating.

The NOXP radar deployed at approximately 2017 UTC (all times in UTC hereafter) and the DOW radar deployed 10 minutes later at 2027. The tornado formed at approximately 2020 and dissipated at approximately 2042. The tornado formed over land just west of Canton, OK and traveled northeast, crossing north northeastward over Canton Lake and then continuing northward over land on the north-northeast side of the Canton Lake (Figure 1). The reflectivity presentation of the knob of the hook significantly evolved throughout the lifecycle of the tornado, most notably as a function of the type, presence, or lack, of debris present in the radar bins. In particular, while the tornado approached Canton Lake, a debris ball (e.g. Burgess et al. 2002, Bluestein et al. 2007) was detected. When the tornado moved over Canton Lake, the reflectivity structure of the knob exhibited a clear eye, but as the tornado moved northeast of the lake, over wooded land, a prominent debris ball very rapidly, within seconds, replaced the clear eye (Figure 2).

These data provided unique opportunities to (a) document the rapid temporal evolution of the debris signature, (b) compare the dual-polarization fields between two different dual-polarization radar systems, and (c) compare damage incurred to high-resolution mobile radar Doppler velocity observations.

2. RAPID EVOLUTION OF DEBRIS SIGNATURE

Observations were available every 7 seconds from the DOW7 radar from when the tornado was over the lake to when it was over land (Figure 3). Over the lake (2030:31 – 2031:07), the tornado exhibits a clear reflectivity eye with lower Z_{dr} and ρ_{hv} values then in the surrounding hook. When the tornado crossed from underlying water to underlying (wooded) land (2031:14 – 2032:18), the reflectivity in the knob of the hook (debris ball) continued to increase as more debris got lofted. Correspondingly, the Z_{dr} and ρ_{hv} values decreased, indicating increased tumbling (therefore randomly oriented) debris.

3. INTERCOMPARISON OF DUAL-POLARIZATION SIGNATURES BETWEEN DOW7 AND NOXP

Quasi-contemporaneous DOW7 and NOXP data were available approximately every 3 minutes. Comparisons between the Z_{dr} and ρ_{hv} fields, along with Doppler velocity and reflectivity, yielded excellent agreement between the two radars (Figure 4). Both radars exhibited a decrease in Z_{dr} and ρ_{hv} values in the knob of the

hook as the debris ball developed when the tornado moved from over the lake surface to over land surface.

Another rare opportunity to inter-compare very-fine-scale dual-polarization observations between the NOXP and DOW7 radars occurred during the Verification of the Origins of Rotation Experiment (Wurman et al. 2012) during the 13 June 2010 tornado that occurred north of Booker, Texas. A comparison of the dual-polarization characteristics of the low-reflectivity ribbon (LRR; Wurman et al. 2012; Kosiba et al. 2012) was possible (Figure 5). Observations suggest an increase in Z_{dr} and decrease ρ_{hv} in the LRR, perhaps indicating the presence of small drops in this region.

4. DAMAGE SURVEY

A detailed ground damage survey was conducted on the day following the tornado (Figure 6). The degree of damage to damage indicators, such as trees, mobile homes, pre-fabricated homes was assessed and will be compared to radar-measured winds at those locations.

5. SELECT REFERENCES

Bluestein, H.B., M.M. French, R.L. Tanamachi, S. Frasier, K. Hardwick, F. Junyent, A.L. Pazmany, 2007: Close-Range Observations of Tornadoes in Supercells Made with a Dual-Polarization, X-Band, Mobile Doppler Radar. *Mon .Wea. Rev.,* **135**, 1522-1543.

Burgess, D. W., M. A. Magsig, J. Wurman, D. C. Dowell, and Y. Richardson, 2002: Radar observations of the 3 May 1999 Oklahoma City tornado. *Wea. Forecasting*, **17**, 456–471.

Kosiba, K. A., J. Wurman, P. Markowski, Y. Richardson, P. Robinson, and J. Marquis, 2012: Genesis of the Goshen County, Wyoming Tornado on 05 June 2009 during VORTEX2 ., *Mon. Wea. Rev.*, Accepted, in press.

Palmer, R., M.I. Biggerstaff, P. Chilcon, G. Zhang, M. Yeary, J. Crain, T. Yu, Y. Zhang, K. Droegemeier, Y.Hong, A. Ryzhkov, T. Schuur, S. Torres, 2009: Weather Education at the University of Oklahoma – An integrated approach. Bull. Amer. Meteor. Soc., 90, 1277–1282.

Wurman, J., J. M. Straka, E. N. Rasmussen, M. Randall, and A. Zahrai, 1997: Design and deployment of a portable, pencil-beam, pulsed, 3-cm Doppler radar. *J. Atmos. Oceanic Technol.*, **14**, 1502-1512.

Wurman, J., 2001: The DOW mobile multiple Doppler network. Preprints, *30th International Conf. on Radar Meteorology*, Munich, Germany, Amer. Meteor. Soc., 95–97.

Wurman, J., D. Dowell, Y. Richardson, P. Markowski, E. Rasmussen, D. Burgess, L. Wicker, and H. Bluestein, 2012a: The Second Verification of the Origins of Rotation in Tornadoes Experiment: VORTEX2, *Bull. Amer. Meteor. Soc.*, **93**, 1147-70.

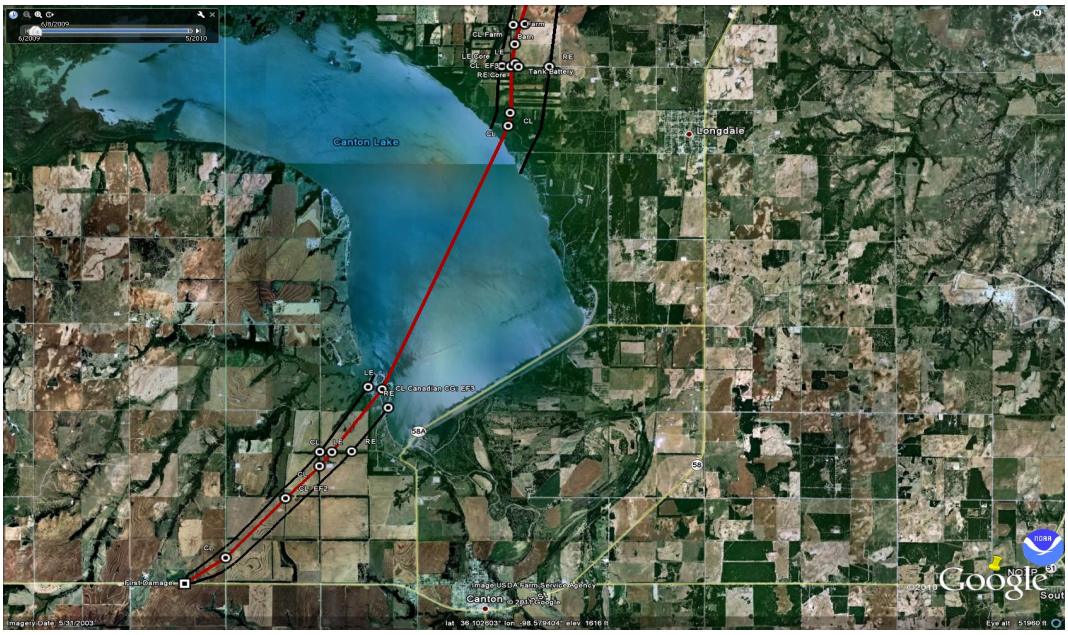

FIGURE 1. Tornado path in red and damage track in black.

(a) 2017 UTC (LAND)

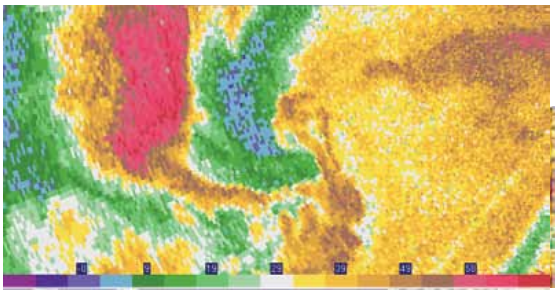

(b) 2024 UTC (LAND)

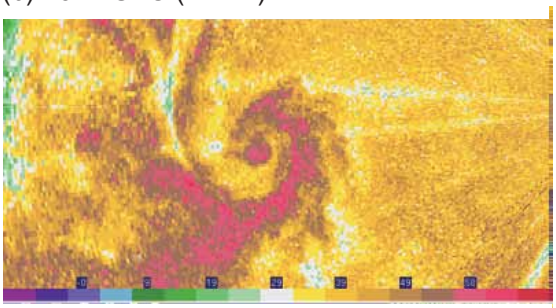

(c) 2029 UTC (LAKE)

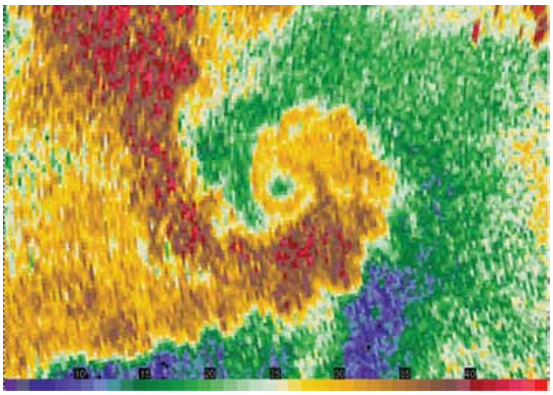

(d) 2032 UTC (LAND)

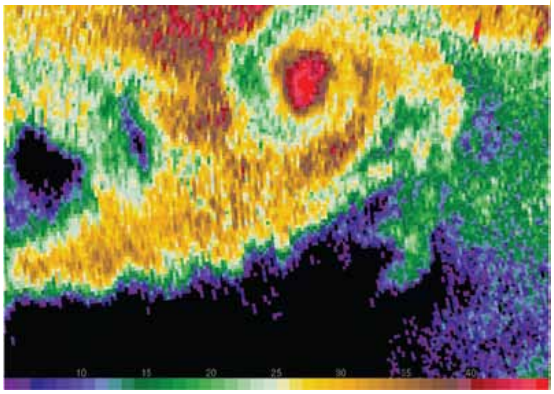

FIGURE 2. Evolution of the reflectivity (a) over land, just prior to tornadogenesis, (b) as the tornado moves off the southwest shore of Canton Lake, (c) when the tornado is over Canton Lake, and (d) when the tornado is back onshore, northwest of Canton Lake. Panels (a) and (b) are the 1° elevation scans from the NOXP radar and panels (c) and (d) are the 0.5 ° elevation scans from the DOW7 radar

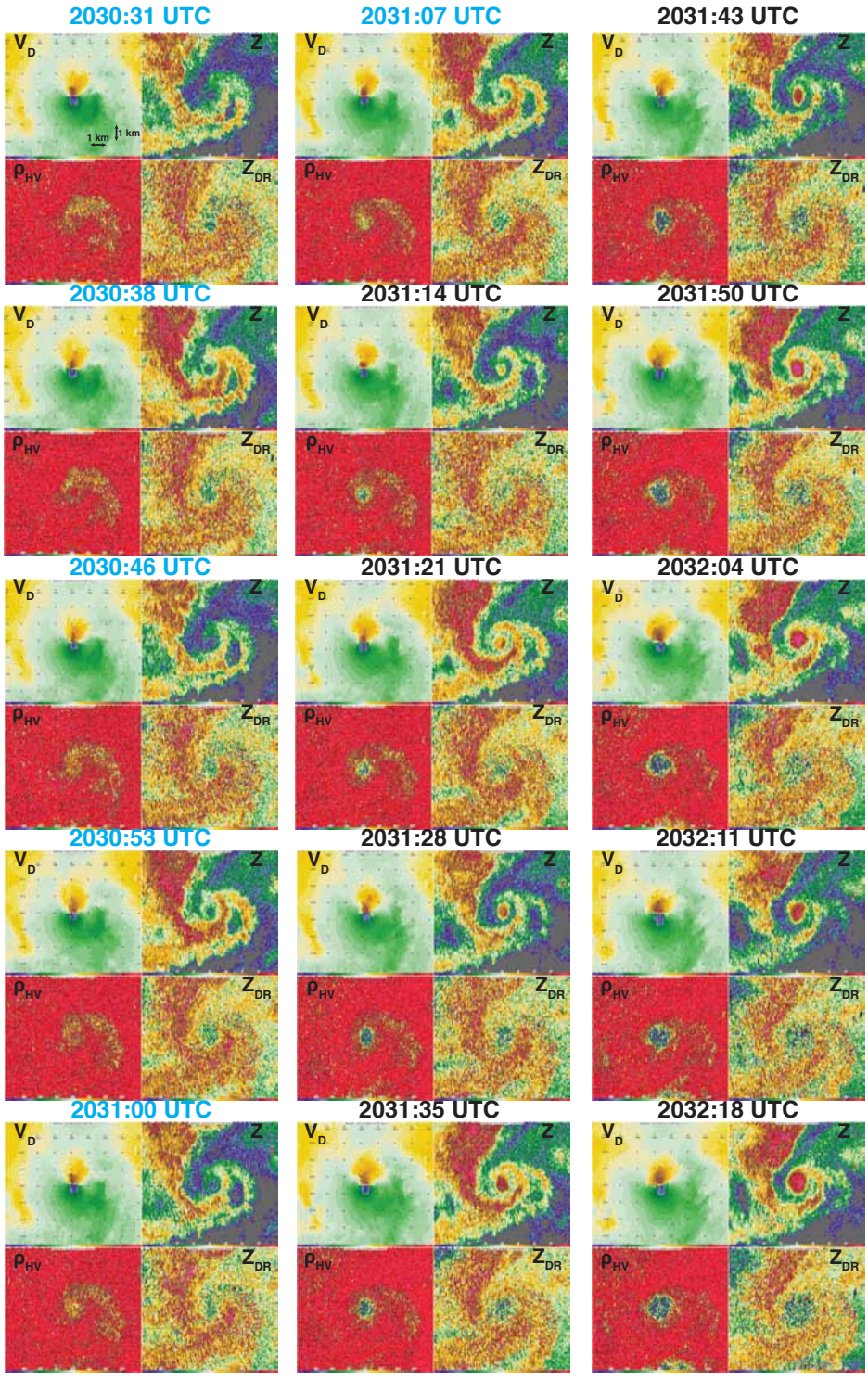

FIGURE 3. Evolution of the Doppler velocity (top left), reflectivity (top right), cross-correlation coefficient (bottom left), and differential reflectivity (bottom right) as observed by the DOW7 radar every 7 seconds. Times in blue (black) indicate when the tornado was over water (land).

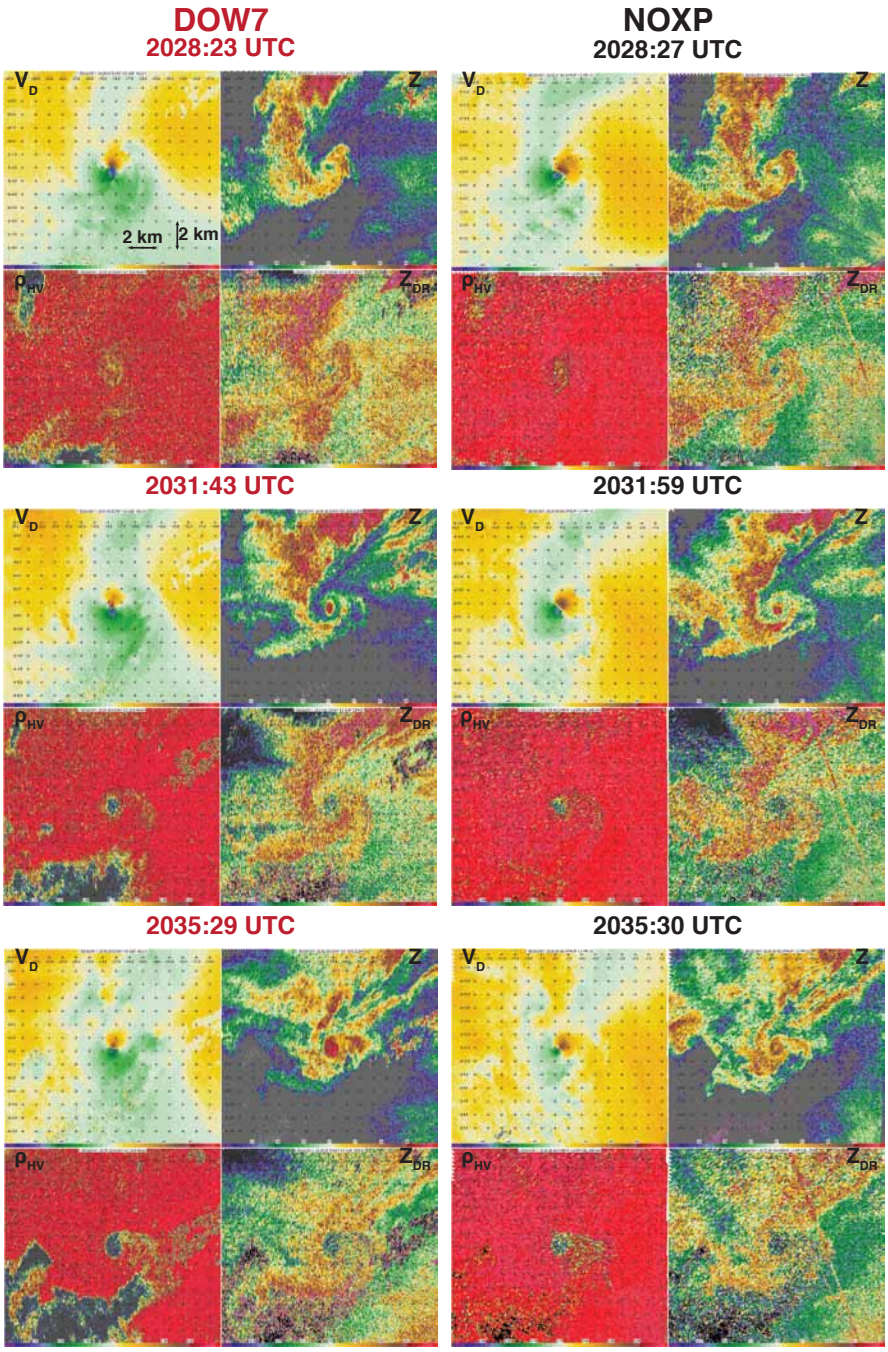

FIGURE 4. Quasi-contemporaneous observations from the DOW7 (red) and NOXP (black) radars of Doppler velocity (top left), reflectivity (top right), cross-correlation coefficient (bottom left), and differential reflectivity (bottom right).

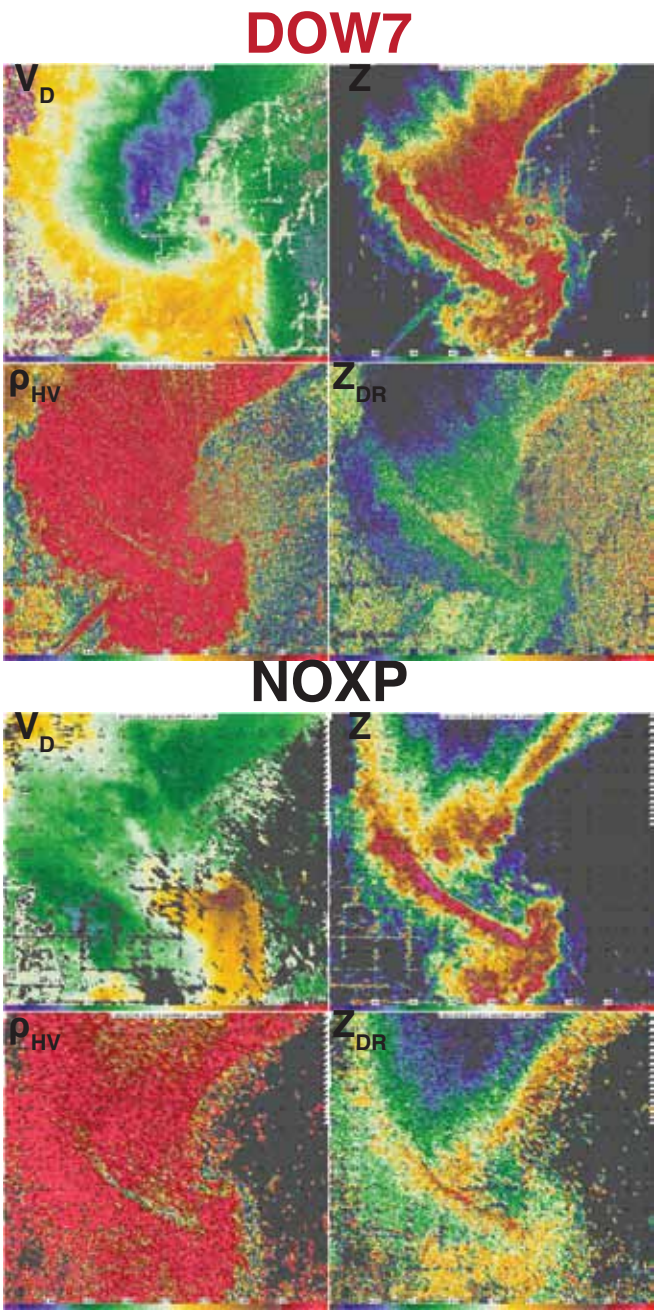

FIGURE 5. Quasi-contemporaneous observations from the DOW7 (red) and NOXP (black) radars of Doppler velocity (top left), reflectivity (top right), cross-correlation coefficient (bottom left), and differential reflectivity (bottom right) from 13 June 2010.

FIGURE 6. Path of tornado (red line) as determined from DOW7 observations and pictures of damage at select locations (blue lines).